Journal of Pharmaceutical and Biomedical Analysis 49 (2009) 587–593

Contents lists available at ScienceDirect

Journal of Pharmaceutical and Biomedical Analysis

journal homepage: www.elsevier.com/locate/jpba

Electrochemical DNA nano-biosensor for the study of spermidine–DNA interaction

Ali Mehdinia[a], S. Habib Kazemi[a], S. Zahra Bathaie[b], Abdolhamid Alizadeh[c], Mojtaba Shamsipur[c], Mir Fazlollah Mousavi[a,*]

[a] Department of Chemistry, Tarbiat Modares University, P.O. Box 14115-175, Tehran, Iran
[b] Department of Clinical Biochemistry, Faculty of Medical Science, Tarbiat Modares University, Tehran, Iran
[c] Department of Chemistry, Razi University, Kermanshah, Iran

ARTICLE INFO

Article history:
Received 30 August 2008
Received in revised form 21 December 2008
Accepted 22 December 2008
Available online 3 January 2009

Keywords:
Nano-biosensor
Self-assembled monolayer
DNA
Spermidine
Differential pulse voltammetry

ABSTRACT

An electrochemical DNA nano-biosensor is prepared by immobilization of double stranded DNA (dsDNA) onto a mixed self-assembled monolayer (SAM) composed of azide- and hydroxyl-terminated thiols. The SAMs- and dsDNA-modified gold electrodes were characterized by cyclic voltammetry (CV) and electrochemical impedance spectroscopy (EIS). The interaction of spermidine with DNA was studied by differential pulse voltammetry at the DNA-modified electrode. The decrease in the guanine oxidation peak current was used to study the interaction. The binding constant (K), obtained by differential pulse voltammetry, was $1.85 \times 10^5\ M^{-1}$. A linear dependence of the guanine peak currents was observed in the range of 1.6–70.4 μM spermidine, with a detection limit of 0.72 μM and $r = 0.994$ by using differential pulse voltammetry.

1. Introduction

Nanostructures, including nanoparticles and nanotubes, have dimensions similar to those of biomolecules such as proteins and DNA. Thus, the combination of nanostructures with biomolecules yields functional nanostructured biointerfaces with synergistic properties and functions [1]. The recent surge of research interest in the bioelectrochemical field is focused on the advanced design and preparation of such potential nanostructured biointerfaces. The use of self-assembly systems, such as Langmuir–Blodgett nanofilms, self-assembled monolayers (SAMs) and layer-by-layer assembled multilayers to the construction of nanostructured biointerfaces for biological applications is of increasing interest [2,3]. Especially, the SAMs have potential applications to the construction of nanodevices for in vivo and ex vivo measurements of metabolites such as DNA [4].

DNA is a special material that tends to participate in the self-assembled polyelectrolyte multilayers due to its large number of negative phosphate groups along the polymeric chain [1]. The DNA (various oligonucleotides) immobilization methods on SAMs have been mainly concentrated on covalent coupling of DNA amine groups with carboxylic groups of short chain thiol SAMs using carbodiimides, generally 1-ethyl-3-(3-dimethyl amino-propyl) carbodiimide hydrochloride (EDC) [5], and N-succinimides, generally N-hydroxysuccinimide (NHS) [6–9] or N-hydroxysulfosuccinimide (NHSS) [10]. However, these methods suffer from some disadvantages as being relatively expensive, time and labor consuming, complicating, losing the DNA activity, and contamination of the sensor by activator reagents [11].

Functionalized monolayers assembled onto the gold surfaces have been widely examined as sensor interfaces [12–14]. One advantage with the self-assembling method over the other surface modifications is that the thickness of the monolayer can be easily controlled by choosing a suitable molecule. The existence of specific interaction between SAMs and the analyte of interest makes the self-assembling method more attractive in comparison with the other modification methodologies. Good selectivity and high sensitivity can be achieved by using of SAMs with appropriate functional groups [15]. It should be noted that more packed monolayers can be obtained by using mixed SAMs compared to single component SAM [16]. In addition, since biomolecules such as DNA has a significantly larger footprint compared to the alkanethiol, other groups can be used for surface dilution in order to spread out the active sites [17,18].

Most electrochemical DNA biosensors are based on the determination of purine oxidation peaks, principally the guanine peak, to monitor the degree of oxidative damage caused to DNA. This is

* Corresponding author. Tel.: +98 21 8288 3474/3479; fax: +98 21 8800 6544.
E-mail addresses: mousavim@modares.ac.ir, mfmousavi@yahoo.com (M.F. Mousavi).

0731-7085/$ – see front matter © 2008 Elsevier B.V. All rights reserved.
doi:10.1016/j.jpba.2008.12.035

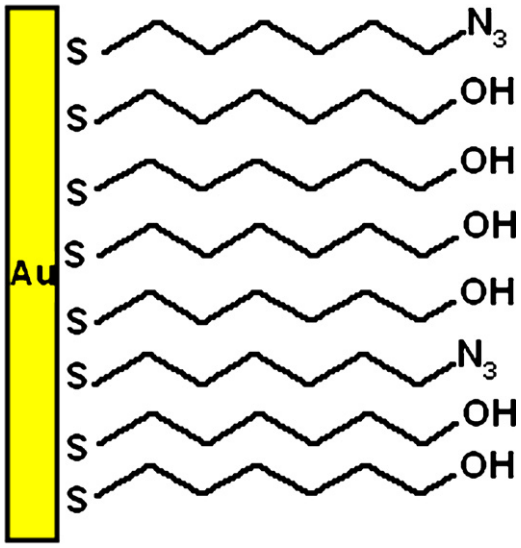

Fig. 1. Schematic representation of mixed SAMs gold modified electrode.

due to the fact that guanine has the lowest oxidation potential of other DNA bases and that its principal oxidation product, 8-oxo-7,8-dihydroguanine, is considered as a useful biomarker of DNA damage by oxidative stress and can be easily quantified by voltammetry [19].

Electrochemical studies of small molecules–DNA interactions by using the low cost, simple and small devices have recently received a good deal of attention, in comparison with the spectroscopic methods [20].

There are several types of reversible interaction of ligands to DNA, including: (i) nonspecific, electrostatic interaction of positively charged ligands with the negatively charged phosphate groups on DNA surface, (ii) binding to one of the two grooves, (iii) intercalation between the stacked base pairs of DNA, (iv) mixed binding through two or more of the above mentioned modes of interaction. In addition, some reagents are known to interact covalently with DNA [21].

Polyamines (putrescine, spermine and spermidine) are involved in the growth of most cells. In cancer cells, polyamine biosynthetic activity and polyamine levels are significantly higher than that in normal cells [22]. Recently, polyamines and their synthetic analogs have been considered as potential anticancer drugs [23].

A few analytical procedures have been developed to study the interaction of spermidine (a recognized cancer marker) and DNA. Spectroscopic and electrophoretic methods such as FT-IR [24], Raman spectroscopy [25] and capillary electrophoresis [24] were used to study the interaction of spermidine and DNA. However, these methods are usually expensive and time-consuming in comparison to the electrochemical methods [26]. The electrochemical methods enable us to evaluate and predict DNA interactions and damage caused to DNA by DNA-binding compounds [27]. Rapid detection, low cost and relatively easy to control the condition is some of the advantages of using electrochemical approaches to study DNA–ligand interaction.

Following our recent studies on the preparing DNA-modified electrodes by adsorption of DNA on glassy carbon electrode [28,29], we recently developed DNA biosensing devices based on a polypyrrole nanofiber-modified platinum electrode [30] and a SAMs-modified gold electrode [31]. In the present study, a new DNA nano-biosensor containing the mixed self-assembled monolayers of 1-azidohexane 6-thiol and 6-mercapto-1-hexanol (with 1:4 ratios, respectively), as a nanostructured substrate, was designed and used for the study of dsDNA–spermidine interactions. The schematic representation of mixed SAMs gold modified electrode is given in Fig. 1. Since SAMs are nanostructures forming a nanometer-scale organic thin-film with a typical thickness of 1–3 nm [32], the proposed modified electrode can be denoted as a DNA nano-biosensor.

2. Experimental

2.1. Chemicals

Calf thymus DNA with high molecular weight was extracted and purified by a method described elsewhere [33] to reach a high purity (an A_{260}/A_{280} = 1.8 indicates that DNA is free from protein and RNA). DNA concentration was spectrophotometrically determined at 260 nm using extinction coefficient of 6600 $(M\,cm)^{-1}$ [21]. All other reagents including spermidine, potassium ferro-/ferricyanide were of analytical grade from Sigma (Buchs, Switzerland). Synthesis of 1-azidohexane 6-thiol was adopted according to a previously published procedure [34]. All solutions were prepared using deionized water.

2.2. Instrumentation

All electrochemical experiments were carried out using an Autolab 30 PGstat controlled with GPES 4.9 and FRA software (Eco-Chemie, Utrecht, The Netherlands). A conventional three electrode one-compartment electrochemical cell with an effective volume of 25 mL containing a gold disc working electrode (2 mm diameter), a 2-cm^2 platinum wire counter electrode, and an Ag/AgCl reference electrode (3 M KCl saturated with AgCl) was used. The differential pulse voltammetric parameters used were: pulse amplitude 50 mV, pulse width 50 ms, scans rate 100 mVs^{-1} and equilibration time 10 s. All potentials are referred to the Ag/AgCl reference electrode. A frequency range of 100 kHz to 0.1 Hz and an AC perturbating signal of 10 mV amplitude were used in impedance measurements. The impedance data were analyzed with a proper electrical equivalent circuit using the complex nonlinear least square (CNLS) method for impedance fitting.

2.3. Formation of mixed SAMs

The working electrode surface was polished with 1 and 0.05 μm alumina powders until a mirror like surface was obtained. Then, it was sonicated in ethanolic solution at least for 10 min. Self-assembled monolayers were prepared by immersing a clean gold electrode in a vial containing 2 mL of an ethanolic solution 1 mM of the mixed of 1-azidohexane 6-thiol and 6-mercapto-1-hexanol (with 1:4 ratios, respectively) for 24–36 h. After the immobilization period, the electrodes were removed from the solution, cleaned with double distillated water, and was dried with a nitrogen stream.

The SAMs-modified gold electrode was stable for more than 3 months in ethanolic solution at 4 °C.

2.4. DNA immobilization

A 1000 μg mL^{-1} stock solution of dsDNA, in a 10 mM Tris buffer solution of pH 7.4 (physiological pH), was prepared, and stored at 4 °C. A 20 μL portion of DNA solution was immobilized onto SAMs-modified gold electrode by drop-cast method and dried for 1 h in desiccator. The DNA-loaded electrode (Au-SAM–DNA) was rinsed with the Tris buffer solution and used for biosensing of spermidine. Differential pulse voltammetric sensing of spermidine was performed in the same buffer as mentioned above. The DNA-modified electrode was stable for more than 7 days in Tris buffer solutions of pH 7.4 at 4 °C, and for performing of a series of experiments on spermidine–DNA interaction.

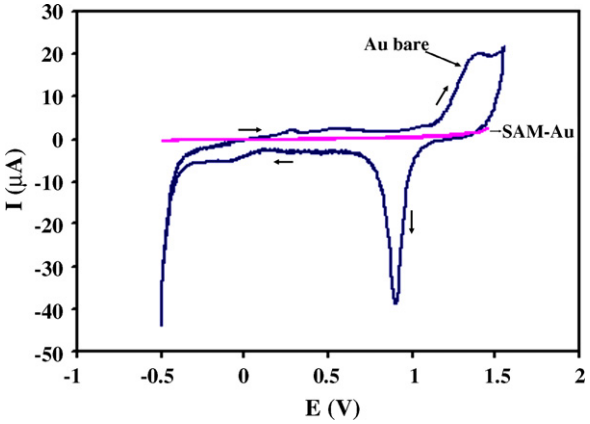

Fig. 2. Comparison of cyclic voltammograms of bare gold electrode (blue lines) and mixed SAMs-modified gold electrode (red lines) in 0.1 M Tris–HCl buffer at a scan rate of 100 mVs^{-1}. Arrows show the direction of potential scan. (For interpretation of the references to color in this figure legend, the reader is referred to the web version of the article.)

3. Results and discussion

3.1. Cyclic voltammetry

Fig. 2 represents the cyclic voltammograms of bare and mixed SAM-modified gold electrodes in Tris buffer solution (pH 7.4). The bare gold electrode shows characteristic anodic and cathodic peaks, which are related to oxidation and reduction of polycrystalline gold metal. In contrast, the cyclic voltammogram for the electrode modified with mixed SAMs shows no significant redox peaks, which can be explained by the complete blocking of the redox reactions and completely coverage of the electrode surface by the SAMs.

The mixed SAMs on the gold surface were characterized by cyclic voltammetry (CV) using $[Fe(CN)_6]^{3-/4-}$ as an electroactive probe. As shown in Fig. 3, a characteristic reversible redox cycle was observed for the unmodified electrode. However, the redox peaks disappeared completely after treatment with mixed SAMs, proving that the dielectric layer on the electrode surface was fully isolated and the access to the surface was blocked by the monolayers.

After immobilizing ds-DNA on the surface of SAMs-modified gold electrode, the effect of scan rates, in the range of 10–200 mVs^{-1}, on the electrochemical response of adsorbed dsDNA was studied. As shown in Fig. 4, with increasing scan rate, the oxidation peak current increased gradually and the oxidation peak potential shifted towards more positive potentials. A linear relationship between the oxidation peak current and the scan rate was established as an indication of a surface confined process. The linear regression equation was expressed as I_p (μA) = 0.002υ (mV s^{-1}) + 0.19 (n = 9, r = 0.997). The mechanism of immobilization ds-DNA onto the mixed-SAMs can be attributed to the electrostatic interaction between positively charged azide groups of SAMs and the negatively charged phosphate groups of DNA.

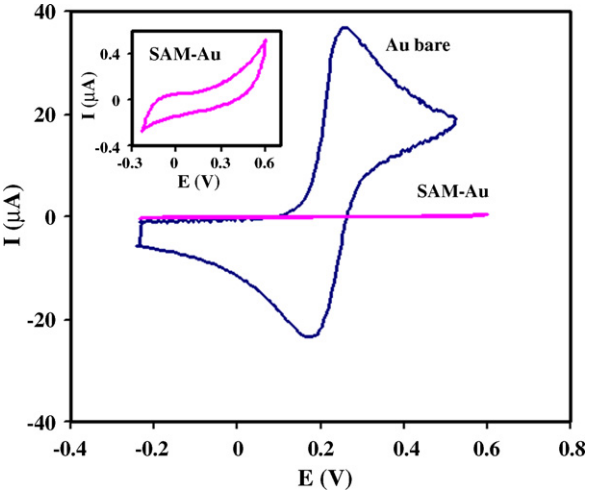

Fig. 3. Typical cyclic voltammograms of 1 mM $[Fe(CN)_6]^{3-/4-}$ at bare and SAMs-modified gold electrodes in 0.1 M Tris–HCl buffer at a scan rate of 100 mVs^{-1}.

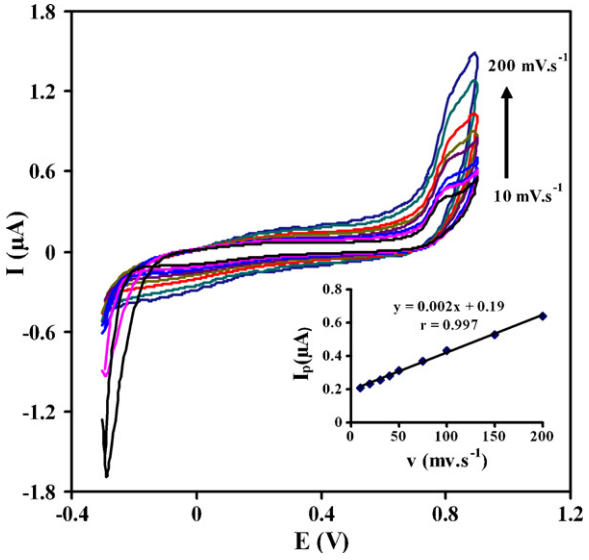

Fig. 4. Cyclic voltammograms of DNA–SAM-Au electrode at scan rates of 10–200 mV s^{-1} in 0.1 M Tris–HCl buffer solution. Inset: plot of the oxidation peak current of guanine against the potential scan rate.

3.2. Impedance measurements

Electrochemical impedance spectroscopy (EIS), as a powerful technique, provides information about the barrier properties and is also sensitive to the interfacial electron transfer as revealed in the characterization of biomolecules [35]. Thus, in this work, EIS was used to describe the immobilizing of dsDNA on the SAMs surface. The electron transfer at SAM-modified electrodes is expected to occur either by tunneling through the barrier or through the defect sites in the barrier. The EIS measurements were performed in the presence of a equimolar ratio of $[Fe(CN)_6]^{3-/4-}$ pair (1 mM each) as electroactive probes. Fig. 5A–C shows the electrochemical impedance spectra (Nyquist, phase and magnitude Bode plots, respectively) for the SAMs- and dsDNA–SAM-modified electrodes at 0.2 V vs. Ag/AgCl. The EIS behavior appeared as a semicircle, corresponding to the electron transfer process, was then modeled with the equivalent circuit (shown the inset of Fig. 5A) consisting of a solution resistance (R_s), a charge-transfer resistance (R_{ct}) and a constant phase element (CPE). The diameter of the semicircle represents the charge-transfer resistance (R_{ct}) at the electrode surface. In this circuit, a CPE was introduced instead of pure capacitance to model the capacitive behavior of the electrode/electrolyte interface.

As shown in Fig. 5A, the diameter of the semicircle, indicating the corresponding R_{ct}, increased for the case of DNA immobilization on the SAMs-modified electrode. This is attributed to increase in the repulsive interaction (electrostatic and steric) between the redox probes and the electrode surface; the repulsion impedes the charge-transfer through the interface. These results are in good agreement with the results of cyclic voltammetry represented in Fig. 3.

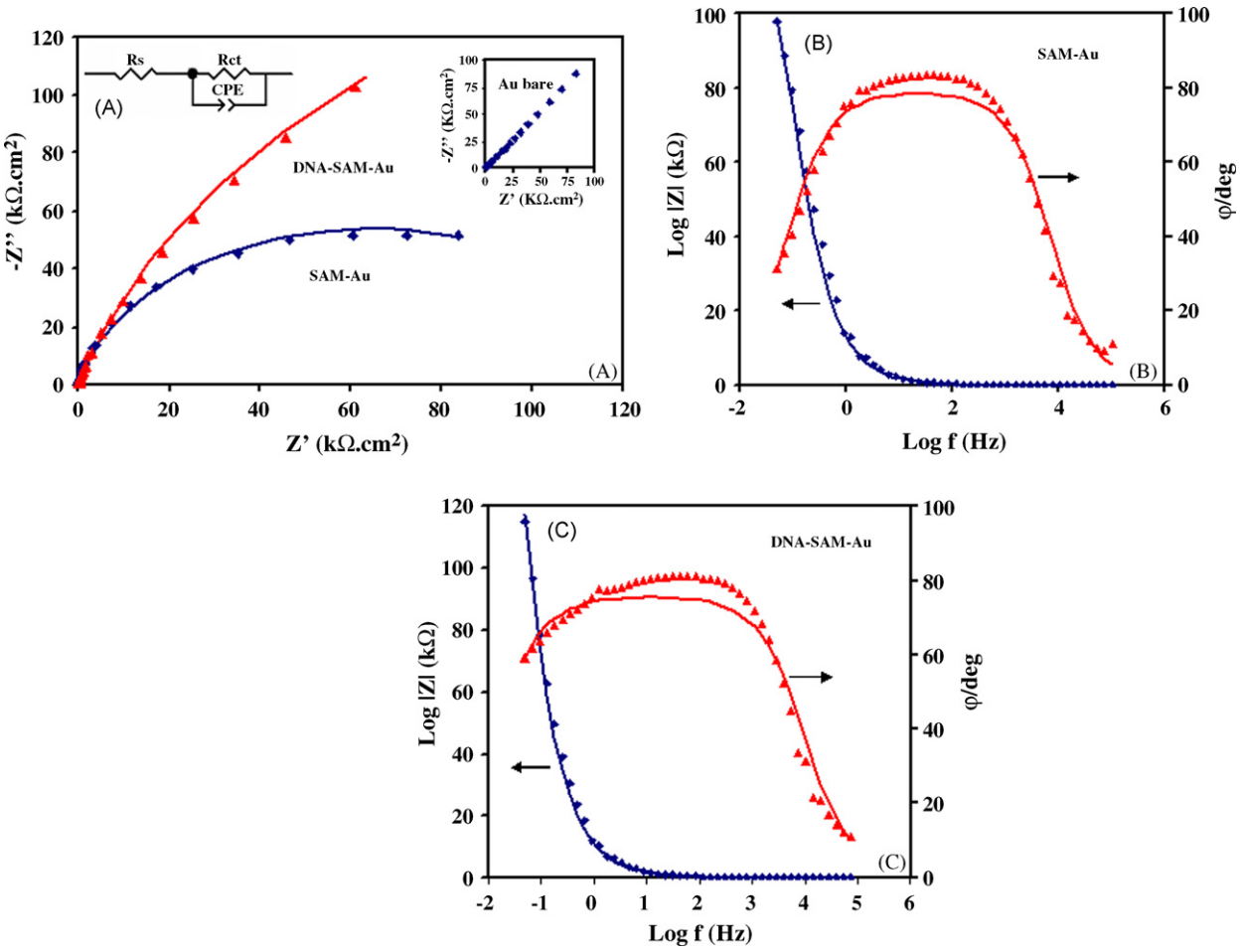

Fig. 5. Nyquist (A) and phase and magnitude Bode plots (B and C) of SAM-Au and DNA–SAM-Au modified electrodes and bare gold electrode in 0.1 M Tris–HCl buffer solution containing 1 mM of $[Fe(CN)_6]^{3-/4-}$; at 0.2 V bias potential vs. Ag/AgCl. The solid lines represent the fitted values to the proposed equivalent circuit (inset) as described in the text.

The Bode plots (Fig. 5B and C) confirm the occurrence of a one-step charge-transfer process and a relaxation process for both SAM-Au and DNA–SAM-Au-modified electrodes. As shown in Fig. 5B and C the experimental data were fitted to an equivalent circuit, which is shown in the inset of Fig. 5A. It should be considered that the proposed model, more or less, fitted the experimental results. Some deviation in the middle frequency can be attributed to non-ideality of the modified surface. In addition, the errors of the fittings are within the range of 10 percent, which is usual and acceptable for the EIS method.

Based on the Bode diagram, it may be concluded that, at medium frequencies, the interfacial double layer capacitance dominates the frequency spectrum, as evidenced by the large capacitive phase angle. At higher frequencies, the double layer capacitor would pass an ac signal with minimal resistance, resulting in a plateau that corresponds to the solution resistance [36]. Here, the double layer capacitance can be modeled by a CPE, where $n < 1$ is a factor used to account for the depression in the semicircle because of distribution in relaxation processes at the electrode–electrolyte interface, as well as inhomogeneities in the modified surface. After immobilizing of DNA on the modified electrode, some of the changes in both R_{ct} and C_{dl} parameters could be observed in Nyquist and Bode plots.

It is noteworthy to mention that the bare gold electrode presents a typical shape consistent with the equivalent circuit for a simple redox reaction: a semicircle in the high frequency domain characteristic of an interfacial charge-transfer mechanism (which can be seen with broadening of Fig. 5A inset) and a straight line with a slope near unity in the low frequency domain characteristic of a semi-infinite diffusion process. Table 1 represents the electrical parameters obtained by fitting the experimental results with the proposed equivalent circuit. The charge-transfer resistance calculated from the semicircle diameter for bare gold electrode was approximately about 1 Ω (not shown here). The monolayers assembled on the electrode surface establish a way to improve the interfacial electron transfer and the charge-transfer resistance increases with the film thickness.

3.3. Surface coverage of the modified electrodes

The packing density and structure of the monolayer can be understood by (i) measuring the capacitance, (ii) determining the surface coverage by reductive desorption and (iii) studying the voltammetric response of the SAM-modified electrodes toward

Table 1
Fitting values of the equivalent circuit elements taken by Zview software for different electrodes.

Electrode	CPE[a] (μF cm^{-2})	n[b]	R_{ct} (kΩ)
SAM-Au electrode	6.1	0.88	91.2
DNA–SAM-Au electrode	14.6	0.88	145.3

[a] Capacitance of CPE element.
[b] Exponent of CPE element.

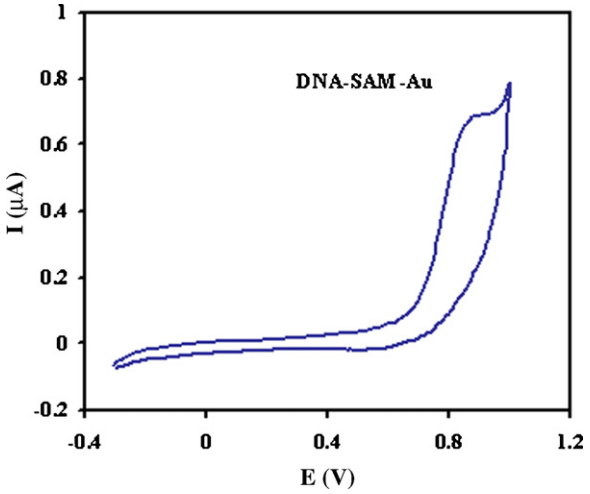

Fig. 6. Typical cyclic voltammograms of DNA–SAM-Au electrode in 0.1 M Tris–HCl buffer solution at a scan rate of 50 mV s^{-1}.

hydrophilic and hydrophobic redox probes [14]. However, a relatively simple method suggested by Finklea and co-workers [37], and extended by Fawcett and Janek [38], assumes that the diffusion to pinhole sites is planar. Considering the above assumption, Eq. (3) can be used for the evaluation of fractional surface coverage of the SAMs-modified electrode:

$$\theta = 1 - \left(\frac{R_{ct}^{Au}}{R_{ct}^{SAM}}\right) \quad (3)$$

where R_{ct}^{Au} and R_{ct}^{SAM} are the charge-transfer resistance values for bare and SAMs-modified electrode, respectively. Since, in our case, the R_{ct} is changed from approximately 1 Ω to more than 82.7 kΩ (see Table 1), the fractional coverage estimated from Eq. (3) is very close to unity, which is higher than the fractional surface coverage obtained in our previous work for single component azide-terminated SAM (0.9999) [31].

On the other hand, Eq. (4) can be used to estimate the DNA layer thickness from the capacitance values [39]:

$$d_i = \frac{\varepsilon_o \varepsilon_i A}{C} \quad (4)$$

where d_i is the thickness of the ith layer, C is the capacitance, ε_o is the permittivity of free space, ε_i is the dielectric constant of the layer, and A is the electrode area. The effective DNA film thickness can be calculated assuming that the CPE is an ideal capacitor and the permittivity of the DNA film is 1 F m^{-1}. Under these assumptions, the effective thickness for the dsDNA was estimated as 19.0 nm.

The adsorbed amount of dsDNA on the surface of SAMs-modified electrode was further calculated by the following equation [40]:

$$\Gamma = \frac{Q}{nFA} \quad (5)$$

where n is the number of electrons transferred, F (C mol^{-1}) is the Faraday's constant, A (cm^2) is the area of the electrode, Γ (mol cm^{-2}) is the surface concentration of the electroactive substance (here it is guanine base), Q (C) is the peak area (calculated by the charges). The charge (Q) under the guanine oxidative peak obtained from the cyclic voltammogram of DNA–SAM-Au electrode as shown in Fig. 6. Based on the obtained value of the electric charge (4.6×10^{-6} C) and surface area (0.0314 cm^2) the average surface concentration of DNA on SAM-modified gold electrode was evaluated as 1.52×10^{-9} mol cm^{-2}. A comparison between the surface concentration of DNA on the azide-terminated SAMs (1.41×10^{-9} mol cm^{-2}) [31] and that on the mixed azide-hydroxyl-terminated SAMs (1.52×10^{-9} mol cm^{-2}) shows a significant enhancement in the latter case.

It should be noticed that the surface coverage obtained in this work (1.52×10^{-9} mol cm^{-2}) is larger than that of the commonly monolayer absorption values reported in the literature (10^{-10} to 10^{-11} mol cm^{-2}) [41,42]. This is most possibly due to the more packed surface structure of the SAM which results in increased adsorption capacity of the surface for dsDNA [43,44].

3.4. Spermidine–DNA interaction

Fig. 7A shows the interaction of spermidine with the DNA-modified electrode studied by differential pulse voltammetry (DPV) in 0.1 M Tris–HCl buffer solution at physiological pH (7.4), by using different concentrations of spermidine. It was found that the guanine peak current decreased with an increase in the spermidine concentration. A calibration curve (Fig. 7B) was obtained in the concentration range of 1.6–70.4 μM spermidine. The detection limit from the calibration curve with $r = 0.994$ was 0.72 μM. The variability of the technique using five replicate standards at

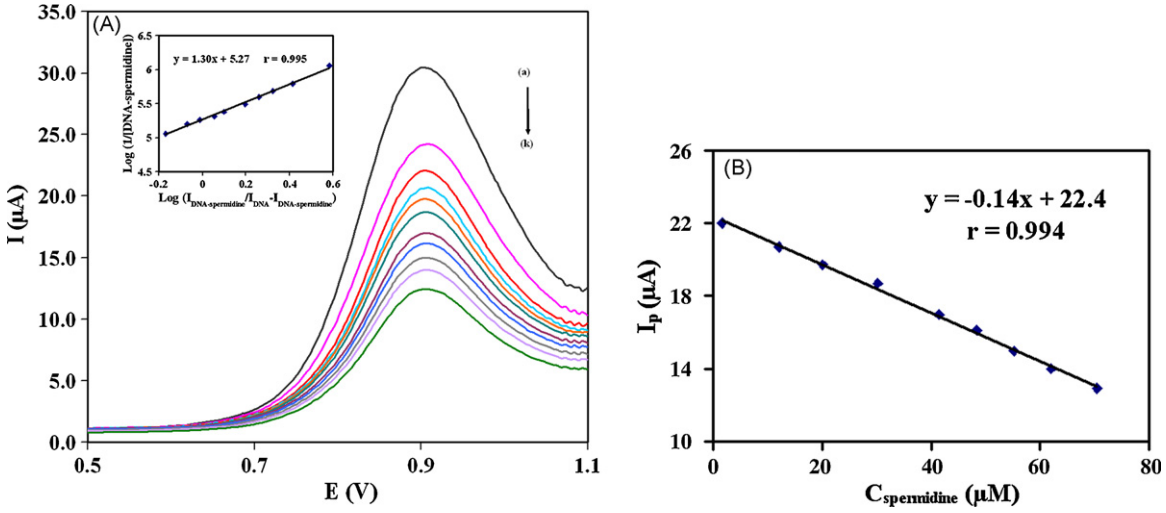

Fig. 7. (A) Differential pulse voltammograms of different concentrations of spermidine in Tris–HCl buffer (pH 7.4). The spermidine concentrations are 0.0, 0.8, 1.6, 2.1, 2.5, 3.2, 4.1, 4.8, 5.5, 6.2 and 8.7 μM (a–k, respectively). Inset: Log (1/[spermidine]) versus Log ($I_{DNA-spermidine}/I_{DNA} - I_{DNA-spermidine}$) plot for estimation of binding constant, K. (B) Calibration curve for the determination of spermidine (1.6–70.4 μM) at dsDNA-modified electrode by using decrease in the guanine oxidation peak area.

Table 2
Comparison of the analytical performance for determination of spermidine by the proposed method and classical methods.

Technique used	Linearity range (μM)	LOD[a] (μM)	r[b]	Reference
HPLC–MS-MS	0.12–3.42	0.04	0.998	[46]
HPLC–UV	0.21–34.2	0.07	0.998	[47]
CZE[c]	0.05–3	0.03	0.999	[48]
CE[d]	2–200	0.01	0.996	[49]
IC-IPAD[e]	0.7–34.4	0.40	0.999	[50]
DPV	1.6–70.4	0.72	0.994	This work

[a] Limit of detection.
[b] Correlation coefficient.
[c] Capillary zone electrophoresis.
[d] Capillary electrophoresis.
[e] Ion chromatography with integrated pulsed amperometric detection.

two concentration levels of 5 and 50 μM was obtained as 2.6% and 3.3%, respectively. Table 2 compares the analytical performance of parameters for determination of spermidine by the proposed method and the classical methods. As can be seen, the analytical performance of parameters of our method is acceptable in comparison with those of the highly sensitive existing methods.

The decrease in the guanine signal of dsDNA-modified electrode can be attributed to the binding of spermidine to this base. It seems that spermidine can diffuse into the DNA grooves (preferentially minor groove) and shield the DNA's electroactive guanine bases. The value of the binding constant for the interaction of spermidine with DNA can be determined by using Eq. (6). The equation was modified slightly according to the nature of the immobilized molecule by replacing drug with DNA as described by Ibrahim [45], where the author immobilized the drug at the electrode surface:

$$Log\left(\frac{1}{[\text{spermidine}]}\right) = Log\,K + Log\left(\frac{I_{\text{DNA-spermidine}}}{I_{\text{DNA}} - I_{\text{DNA-spermidine}}}\right) \quad (6)$$

where K is the apparent binding constant, I_{DNA} is peak current of immobilized DNA, and $I_{\text{DNA–spermidine}}$ is the peak current of DNA after interaction with spermidine. According to the Eq. (6), a plot of Log (1/[spermidine]) against Log ($I_{\text{DNA–spermidine}}/I_{\text{DNA}} - I_{\text{DNA–spermidine}}$) will result in a straight line (inset of Fig. 7A), the intercept of which being equal to the logarithm of binding constant. The K value thus calculated found to be $1.85 \times 10^5\ M^{-1}$, which is in satisfactory agreement with the previously reported values obtained by affinity capillary electrophoresis (i.e., $1.4 \times 10^5\ M^{-1}$) [24]. The observed differences in the reported values of the binding constant might be due to differences in solution conditions and the studied methods. As it is seen in the literature, both the electrostatic interaction and the direct binding of spermidine with DNA minor grove were reported [24,25].

In our previous works [28,29], using a DNA-modified glassy carbon electrode, we showed that the neutral red bind to dsDNA with an affinity constant equal to $2.76 \times 10^4\ M^{-1}$. Because of the aromatic structure of neutral red, it can intercalate between DNA base pairs. However in the present work, using a DNA-modified gold electrode the interaction of spermidine with DNA was investigated. The guanine oxidation peak in DNA was probed for the monitoring of its interaction with spermidine and an affinity constant equal to $1.85 \times 10^5\ M^{-1}$ was obtained. The nature of this interaction is mainly the groove-binding mode. Although, the electrodes used in these methods are different, but by comparison of the binding constants, it seems that the affinity of spermidine-for interaction with DNA is more than the neutral red, may be due to its positive charges that potentiates its interaction with DNA.

4. Conclusions

Mixed azide- and hydroxy-terminated SAMs have been employed as a good nanostructured platform for the construction of a novel DNA nano-biosensor. The spermidine–DNA interaction was studied by the proposed dsDNA nano-biosensor. Two different modes of electrostatic and minor groove bindings can be deduced using the electrochemical studies. The binding constant determined by differential pulse voltammetry was in satisfactory agreement with the previously reported data. The advantages of the proposed nano-biosensor are rapid detection, low cost, relatively broad dynamic range and low detection limit, as well as its effectiveness and easy to use at physiological pH.

References

[1] D. Chen, G. Wang, J. Li, J. Phys. Chem. C 111 (2007) 2351–2367.
[2] L.J.C. Jeuken, N.N. Daskalakis, X. Han, K. Sheikh, A. Erbe, R.J. Bushby, S.D. Evans, Sens. Actuators B-Chem. 124 (2007) 501–509.
[3] M. Shamsipur, S.H. Kazemi, A. Mehdinia, M.F. Mousavi, H. Sharghi, Electroanalysis 20 (5) (2008) 513–519.
[4] F. Caruso, E. Rodda, D.N. Furlong, K. Niikura, Y. Okahata, Anal. Chem. 69 (1997) 2043–2049.
[5] F. Nakamura, E. Ito, T. Hayashi, M. Hara, Colloid Surf. A 284–285 (2006) 495–498.
[6] K. Kerman, D. Ozkan, P. Kara, B. Meric, J.J. Gooding, M. Ozsoz, Anal. Chim. Acta 462 (2002) 39–47.
[7] E. Huang, F. Zhou, L. Deng, Langmuir 16 (2000) 3272–3280.
[8] D. Ozkan, A. Erdem, P. Kara, K. Kerman, J.J. Gooding, P.E. Nielsen, M. Ozsoz, Electrochem. Commun. 4 (2002) 796–802.
[9] N. Wrobel, W. Deininger, P. Hegemann, V.M. Mirsky, Colloid. Surf. B 32 (2003) 157–162.
[10] O.A. Loaiza, S. Campuzano, M. Pedrero, J.M. Pingarron, Talanta 73 (2007) 838–844.
[11] R. Karimi-Shervedani, A. Hatefi-Mehrjardi, Sens. Actuators B-Chem. 126 (2007) 415–423.
[12] R.Y. Lai, D.S. Seferos, A.J. Heeger, G.C. Bazan, K.W. Plaxco, Langmuir 22 (25) (2006) 10796–10800.
[13] G.A. Campbell, R. Mutharasan, Anal. Chem. 78 (7) (2006) 2328–2334.
[14] C.R. Yonzon, E. Jeoung, S. Zou, G.C. Schatz, M. Mrksich, R.P. Van Duyne, J. Am. Chem. Soc. 126 (39) (2004) 12669–12676.
[15] S. Behera, C.R. Raj, Sens. Actuators B-Chem. 128 (2007) 31–38.
[16] A.M.O. Brett, J.A.P. Piedade, L.A. Silva, V.C. Diculescu, Anal. Biochem. 332 (2004) 321–329.
[17] C.D. Bain, J. Evall, G.M. Whitesides, J. Am. Chem. Soc. 111 (1989) 7155–7164.
[18] Th. Wink, S.J. van Zuilen, A. Bult, W.P. van Bennekom, Analyst 122 (1997) 43R–50R.
[19] M. Satjapipat, R. Sanedrin, F. Zhou, Langmuir 17 (2001) 7637–7644.
[20] L.R. Wang, R.X. Wang, L.Z. Yang, G.H. Lu, J. Electroanal. Chem. 585 (2005) 214–219.
[21] S.Z. Bathaie, A. Bolhasani, R. Hoshyar, B. Ranjbar, F. Sabouni, A.A. Moosavi-Movahedi, DNA Cell Biol. 26 (2008) 533–540.
[22] N. Shah, T. Thomas, A. Shirahata, L.H. Sigal, T.J. Thomas, Biochemistry 38 (1999) 14763–14774.
[23] T. Thomas, T. Thomas, J. Cell Mol. Life Sci. 58 (2001) 244–258.
[24] A.A. Ouameur, H.A. Tajmir-Riahi, J. Biol. Chem. 279 (40) (2004) 42041–42054.
[25] J. Ruiz-Chica, M.A. Medina, F. Sanchez-Jimenez, F.J. Ramirez, Biophys. J. 80 (2001) 443–454.
[26] E.S. Gil, S.H.P. Serrano, E.I. Ferreira, L.T. Kubota, J. Pharmaceut. Biomed. 29 (2002) 579–584.
[27] S. Rauf, J.J. Gooding, K. Akhtar, M.A. Ghauri, M. Rahman, M.A. Anwar, A.M. Khalid, J. Pharmaceut. Biomed. 37 (2005) 205–217.
[28] H. Heli, S.Z. Bathaie, M.F. Mousavi, Electrochem. Commun. 6 (2004) 1114–1118.
[29] H. Heli, S.Z. Bathaie, M.F. Mousavi, Electrochim. Acta 51 (2005) 1108–1116.
[30] K. Ghanbari, S.Z. Bathaie, M.F. Mousavi, Biosens. Bioelectron. 23 (2008) 1825–1831.
[31] A. Mehdinia, S.H. Kazemi, S.Z. Bathaie, A. Alizadeh, M. Shamsipur, M.F. Mousavi, Anal. Biochem. 375 (2008) 331–338.
[32] J.C. Love, L.A. Estroff, J.K. Kriebel, R.G. Nuzzo, G.M. Whitesides, Chem. Rev. 105 (2005) 1103–1169.
[33] S.Z. Bathaie, A.A. Moosavi-Movahedi, A.A. Saboury, Nucleic Acids Res. 27 (1999) 1001–1005.
[34] E.J. Oneil, K.M. DiVittorio, B.D. Smith, Org. Lett. 9 (2007) 199–202.
[35] M. Shamsipur, S.H. Kazemi, M.F. Mousavi, Biosens. Bioelectron. 24 (2008) 104–110.
[36] A.R. Abdur-Rahman, C.-M. Lo, S. Bhansali, Sens. Actuators B-Chem. 118 (2006) 115–120.
[37] H.O. Finklea, D. Snider, J. Fedyk, E. Sabatani, Y. Gafni, I. Rubinestein, Langmuir 9 (1993) 3660–3667.
[38] R. Fawcett, R. Janek, Langmuir 14 (1998) 3011–3018.
[39] G.S. Pomales, L.S. Rodriguez, N.E.R. Velez, C.R. Cabrera, J. Electroanal. Chem. 611 (2007) 80–86.

[40] M. Yousef-Elahi, H. Heli, S.Z. Bathaie, M.F. Mousavi, J. Solid State Electrochem. 11 (2007) 273–282.
[41] F.R.R. Teles, L.P. Fonseca, Talanta 77 (2008) 606–623.
[42] X.Q. Ding, J. Li, J. Hu, Q. Li, Anal. Biochem. 339 (2005) 46–53.
[43] I. Karamollaoglu, H.A. Oktem, M. Mutlu, doi:10/1016/j.bej.2008.11.011.
[44] J. Rivera-Gandía, R.M. Georgiadis, C.R. Cabrera, J. Electroanal. Chem. 621 (2008) 75–82.
[45] M.S. Ibrahim, Anal. Chim. Acta 443 (2001) 63–72.
[46] F. Gosetti, E. Mazzucco, V. Gianotti, S. Polati, M.C. Gennaro, J. Chromatogr. A 1149 (2007) 151–157.
[47] M.D. Koppang, M. Witek, J. Blau, G.M. Swain, Anal. Chem. 71 (1999) 1188–1195.
[48] L.Y. Zhang, X.C. Tang, M.X. Sun, J. Chromatogr. B 820 (2005) 211–219.
[49] X. Sun, X. Yang, E. Wang, J. Chromatogr. A 1005 (2003) 189–195.
[50] B.M.D. Borba, J.S. Rohrer, J. Chromatogr. A 1155 (2007) 22–30.